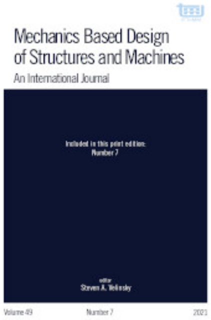

Taylor & Francis
Taylor & Francis Group

Mechanics Based Design of Structures and Machines

An International Journal

ISSN: (Print) (Online) Journal homepage: https://www.tandfonline.com/loi/lmbd20

Modal analysis of cracked FGM beam with piezoelectric layer

Nguyen Tien Khiem, Tran Thanh Hai & Luu Quynh Huong

To cite this article: Nguyen Tien Khiem, Tran Thanh Hai & Luu Quynh Huong (2021): Modal analysis of cracked FGM beam with piezoelectric layer, Mechanics Based Design of Structures and Machines, DOI: 10.1080/15397734.2021.1992775

To link to this article: https://doi.org/10.1080/15397734.2021.1992775

Published online: 28 Oct 2021.

MECHANICS BASED DESIGN OF STRUCTURES AND MACHINES
https://doi.org/10.1080/15397734.2021.1992775

Taylor & Francis
Taylor & Francis Group

Modal analysis of cracked FGM beam with piezoelectric layer

Nguyen Tien Khiem[a,b], Tran Thanh Hai[b], and Luu Quynh Huong[c]

[a]Center for Interdisciplinary Research, Ho Chi Minh City University of Technology (HUTECH), Ho Chi Minh City, Vietnam; [b]Institute of Mechanics, Vietnam Academy of Science and Technology, Ba Dinh, Hanoi, Vietnam; [c]Faculty of Water Resources Engineering, Thuy Loi University, Hanoi, Vietnam

ABSTRACT

The present paper addresses modal analysis of cracked Timoshenko beam bonded with piezoelectric layer. The host beam is made of functionally graded material with the power law and crack appeared in the host beam is modeled by a pair of axial and rotational springs with stiffness calculated from its depth. The piezoelectric layer is represented as a homogeneous Timoshenko beam. Governing equations and general solution for free vibration of the cracked double beam are conducted in the frequency domain. The obtained solution has been used for examining modal parameters of the coupled beam that include natural frequencies, mode shapes and so-called modal sensor charge in dependence on crack parameter, material gradient index and thickness of piezoelectric layer. Analysis of the modal sensor charge in dependence upon crack parameters provides a novel indicator that is expected to be more efficient than the traditional ones for crack detection in functionally graded beam using distributed smart sensors. The theoretical development is validated and illustrated by numerical analysis accomplished for simply supported beam.

ARTICLE HISTORY
Received 17 February 2021
Accepted 9 October 2021

KEYWORDS
Modal analysis; functionally graded material; cracked Timoshenko beam; piezoelectric layer

1. Introduction

Damage detection in general, or crack identification in particularity, is essential problem in the structural health monitoring that has been intensively studied through several latest decades and it was reviewed by numerous authors, for instance, Sohn et al. (2003), Fan and Qiao (2011) and Hou and Xia (2021). Most of researchers in the field of structural health monitoring have agreed to that dynamic behavior or vibration circumstance of a structure provides the most useful tool for diagnosis of potential damages in the structure. However, the conventional approach such as the dynamic testing technique to gather dynamic features necessary for structural health monitoring is limited to collect insufficient data for solving the inverse problem of the structural damage identification. Alternately, many authors (Rao and Sunar 1994; Park et al. 2003; Giurgiutiu 2007; Duan, Wang, and Quek 2010, etc.) have demonstrated that using smart material such as piezoelectric one the structural health monitoring becomes much more advantaged in both its implementation and success in damage detection. This is because of the smart material could be used not only for sensing signal of the structure response as a sensor but also for transmitting load to structure as an actuator. Additionally, the smart transducers are distributed (Tzou and Tseng 1990) and may be permanently installed as components working together with structure of interest (Crawley and De Luis1987). Recent progress in structural health monitoring using distributed

CONTACT Nguyen Tien Khiem nt.khiem55@hutech.edu.vn, ntkhiem@imech.vast.vn
Communicated by Kuang-Hua Chang.

piezoelectric transducers was reported in Winston, Sun, and Annigeri 2000; Bhalla and Soh 2006; Huang, Song, and Wang 2010; Shu 2017; Na and Baek 2018.

Obviously, the use of smart distributed sensor/actuator for structural health monitoring is essentially leading to analysis of structures with smart components. Namely, Wang and Quek (2000) used the sandwich beam model for modal analysis of a Euler-Bernoulli beam embedded with piezoelectric layers and they found that natural frequency of the sandwich beam is function of stiffness and thickness of the piezoelectric layers. Wang and Quek (2002) showed that the buckling and flutter capacities of an elastic column could be enhanced by using piezoelectric patches bonded to both sides of the column as actuators with an applied voltage. Wang, Duan, and Quek (2004) revealed an effect of a piezoelectric patch bonded to a beam on its natural frequency and demonstrated an interesting fact that piezoelectric patch used as an actuator could restore the healthy condition of a cracked beam. Zhao, Wu, and Wang (2017) proposed a procedure for crack identification in beam based on the crack-induced frequency change that is amplified by applying a feedback voltage output from piezoelectric sensor through collocated actuator. The so-called Electro-Mechanical Impedance (EMI) method was developed in Ritdumrongkul and Fujino 2007; Wang, Song, and Zhu 2015; Wang et al. 2020 for crack identification in beam using piezoelectric transducers. The authors have concluded that the EMI is sensitive to local damage such as crack only at the high frequency range and when the transducer is positioned near the damage location. Therefore, using a piezoelectric layer bonded to a beam structures as full-length distributed sensor is promising idea to gather diagnostic signal for damage detection that is investigated in the present study for functionally graded beam with crack.

Various problems in dynamics of functionally graded beams and plates were studied in the widespread literature, for instance, Li 2008; Sina, Navazi, and Haddadpour 2009; Larbi et al. 2013; Hu and Zhang 2011; Su and Banerjee 2015; Wang, Liang, and Jin 2017. Numerous works are devoted also to study vibrations of the beams with localized damages such as cracks, for example, Yang and Chen 2008; Akbas 2013; Aydin 2013; Khiem, Tran, and Nam 2020. Some procedures were proposed by Yu and Chu (2009); Banerjee, Panigrahi, and Pohit (2016) and Khiem and Huyen (2017) to detect cracks in functionally graded beams with natural frequencies measured by the conventional technique of modal testing. There are few studies reported on smart structures made of Functionally Graded Material (FGM). Namely, stability of FGM Timoshenko beam embedded by the top and bottom piezoelectric layers has been investigated by Khorramabadi and Nezamabadi (2010) and it is found a significant effect of both the piezoelectric actuators and FGM parameters on the critical buckling loads. Li, Feng, and Cai (2014) even proposed a model of functionally graded piezoelectric beam for its vibration analysis and revealed the increase of natural frequency and decrease of electric potential with increasing gradient index of the material. Bendine et al. 2016 studied the problem for active vibration control of functionally graded beams with upper and lower surface-bonded piezoelectric layers by the finite element method. Khiem, Hai, and Huong 2020 examined the effect of piezoelectric patches on natural frequencies of undamaged functionally graded beam. However, to the authors knowledge, the damage detection for FGM structures using smart sensor/actuator has not received adequate concern.

The above short overview shows that using smart material such as piezoelectric one as distributed sensor for structural damage detection in composite structures (Golewski 2021) such as FGM structures is necessary, but it has not been paid adequate attention. The most important issue for solving the problem of the damage identification is modeling and analysis of damaged structures coupled with smart sensors. Thus, the present paper addresses modal analysis of cracked FGM beam with a bonded piezoelectric layer. Governing equations and general solution for free vibration of the coupled smart beam are conducted and used for examining modal parameters such as natural frequencies, mode shapes and so-called modal sensor charge generated in the piezoelectric layer under the vibration modes in dependence upon crack depth and location. This study can be distinguished from other ones first by that a piezoelectric sensor used to

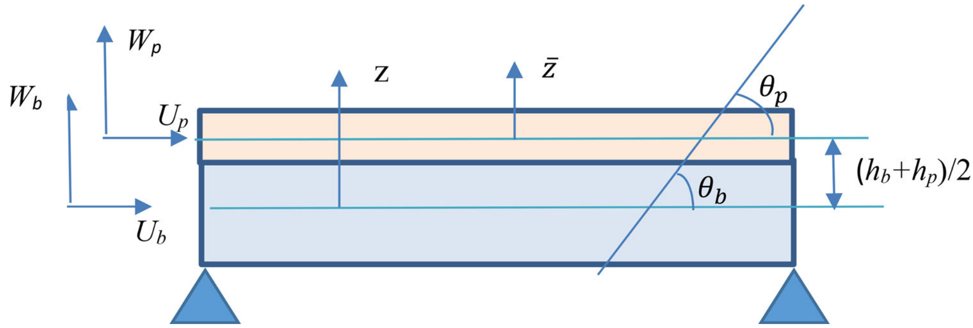

Figure 1. FGM beam element with piezoelectric layer.

gather vibration behavior of an FGM beam needed for its crack identification is distributed over the beam length and bonded to the beam as it's a structural layer. Secondly, while the most of earlier authors intended to use the conventional modal parameters for solving the crack detection problem, this study aimed directly to analysis of the sensor output charge with purpose to use it as an indicator for crack detection in FGM beam. The charge is much more easily to measure than the EMI or extracted from those natural frequencies.

2. Governing equations

Consider an FGM beam of length L, cross sectional area $A_b = b \times h_b$ (Figure 1). It is assumed that the material properties of the beam vary along the thickness direction by the power law distribution as follows

$$\Re(z) = \Re_b + (\Re_t - \Re_b)(z/h + 0.5)^n; -h_b/2 \le z \le h_b/2, \tag{1}$$

where $\Re$ stands for Young's, shear modulus and material density E, G, ρ; subscripts t and b denote the top and bottom material respectively; n is power law exponent; z is ordinate of point along the beam height from the mid plane. Assuming small deformation in the framework of Timoshenko beam theory, the constituting equations for the beam at section x are

$$u(x,z,t) = u_0(x,t) - (z - h_0)\theta(x,t) \ ; \ w(x,z,t) = w_0(x,t);$$
$$\sigma_x = E(z)\varepsilon_x; \ \tau_{xz} = \kappa G(z)\gamma_{xz}; \varepsilon_x = \partial u_0/\partial x - (z - h_0)\partial\theta/\partial x; \gamma_{xz} = \partial w_0/\partial x - \theta, \tag{2}$$

where $u(x,z,t), w(x,z,t)$ are axial and transverse displacements in cross-section at x; $u_0(x,t), w_0(x,t)$ are the displacements on the neutral plane and θ is rotation of the cross-section; $\varepsilon_x, \gamma_{xz}, \sigma_x, \tau$ are deformation and strain components; κ is geometry correction factor; h_0 is acknowledged as exact position of neutral plane measured from the beam midplane. Based on the condition for neutral plane of the FGM beam, the actual position of neutral axis is calculated as

$$h_0 = n(r_e - 1)h/2(n + 2)(n + r_e); r_e = E_t/E_b. \tag{3}$$

Using the constitutive equations (2) strain energy of the beam is calculated as

$$\Pi_b = \left(1/2\right)\int\int\int(\sigma_x\varepsilon_x + \tau_{xz}\gamma_{xz})dV_b = (1/2)\int\int\int[E(z)\varepsilon_x^2 + \kappa G(z)\gamma_{xz}^2]dV_b =$$
$$= (1/2)\int_0^L \left\{A_{11}u_0'^2 - 2A_{12}u'_0\theta' + A_{22}\theta'^2 + A_{33}(w_0' - \theta)^2\right\}dx, \tag{4}$$

where comma denotes derivative with respect to spatial variable x and

$$A_{11} = \int_A E(z)dA = bhE_b\varphi_1(r_e, n); A_{12} = \int_A E(z)(z - h_0)dA = bh^2E_b\varphi_2(r_e, n);$$

$$A_{22} = \int_A E(z)(z - h_0)^2dA = bh^3E_b\varphi_3(r_e, n); A_{33} = \kappa\int_A G(z)dA = bh\kappa G_b\varphi_1(r_g, n); \tag{5}$$

$$\varphi_1(x, n) = (x + n)/(1 + n); \varphi_2(x, n) = (2x + n)/2(2 + n) - \alpha(x + n)/(1 + n);$$

$$\varphi_3(x, n) = (3x + n)/3(3 + n) - \alpha(2x + n)/2(2 + n) + \alpha^2(x + n)/(1 + n);$$

$$r_\rho = \rho_t/\rho_b; r_e = E_t/E_b; r_g = G_t/G_b; \alpha = 1/2 + h_0/h_b.$$

On the other hand, kinetic energy of the beam is

$$T_b = \left(1/2\right)\iiint \rho(\dot{u}^2 + \dot{w}^2)dV = (1/2)\int_0^L \left\{I_{11}\dot{u}_0^2 - 2I_{12}\dot{u}_0\dot{\theta} + I_{22}\dot{\theta}^2 + I_{11}\dot{w}_0^2\right\}dx \tag{6}$$

with

$$I_{11} = \int_A \rho(z)dA = bh_b\rho_b\varphi_1\left(r_\rho, n\right); I_{12} = \int_A \rho(z)(z - h_0)dA = bh_b^3\rho_b\varphi_2(r_\rho, n\Big); \tag{7}$$

$$I_{22} = \int_A \rho(z)(z - h_0)^2dA = bh_b^3\rho_b\varphi_3(r_\rho, n\Big).$$

Let's now consider the piezoelectric layer as a homogeneous Timoshenko beam element, so that constitutive equations can be expressed as

$$u_p(x, \bar{z}, t) = u_{p0}(x, t) - \bar{z}\theta_p(x, t), w_p(x, \bar{z}, t) = w_{p0}(x, t);$$

$$\varepsilon_{px} = u'_{p0} - \bar{z}\theta'_p, \gamma_p = w'_{p0} - \theta_p; \tag{8}$$

$$\sigma_{px} = C_{11}^p\varepsilon_{px} - h_{13}D; \tau_p = C_{55}^p\gamma_p; \quad \in = -h_{13}\varepsilon_{px} + \beta_{33}^pD,$$

where C_{11}^p, h_{13}, β_{33}^p are elastic modulus, piezoelectric and dielectric constants respectively. $\in$ and D are electric field and displacement of the piezoelectric layer.

Perfect bonding of the base beam with the piezoelectric layer is represented by the conditions

$$u\left(x, \frac{h_b}{2}, t\right) = u_p\left(x, -\frac{h_p}{2}, t\right), w(x, h_b/2, t) = w_p\left(x, -h_p/2, t\right), \tag{9}$$

that yield

$$u_{p0} = u_0 - \theta h/2, h = h_b + h_p, w_{p0} = w_0, \theta = \theta_p. \tag{10}$$

Therefore

$$\varepsilon_{px} = u'_0 - (\bar{z} + h/2)\theta', \gamma_p = w'_0 - \theta; \tag{11}$$

and strain and kinetic energies of the layer can be calculated as

$$\Pi_p = \frac{1}{2}\iiint(\sigma_{px}\varepsilon_{px} + \tau_p\gamma_p + \in D)dV_p = \frac{1}{2}\iiint[C_{11}^p\varepsilon_{px}^2 - 2h_{13}D\varepsilon_{px} + C_{55}^p\gamma_p^2 + \beta_{33}^pD^2]dV_p =$$

$$= \left(1/2\right)\int_0^L \left\{C_{11}^pA_pu_0'^2 - C_{11}^pA_phu'_0\theta' + C_{11}^p(I_p + A_ph^2/4)\theta'^2 + C_{55}^pA_p\left(w'_0 - \theta\right)^2\right\}dx-$$

$$-\left(1/2\right)\int_0^L\left\{2h_{13}A_pD(u_0'-h\theta'/2)-\beta_{33}^pA_pD^2\right\}dx; \tag{12}$$

$$T_p=\frac{1}{2}\int\int\int\rho_p\left(\dot{u}_p^2+\dot{w}_p^2\right)dV=\frac{1}{2}\int_0^L\left\{\rho_pA_p\dot{u}_0^2-\rho_pA_ph\dot{u}_0\dot{\theta}+(\rho_pI_p+\rho_pA_ph^2/4)\dot{\theta}^2+\rho_pA_p\dot{w}_0^2\right\}dx,$$

where $A_p=bh_p;\ I_p=bh_p^3/12$. Therefore, total strain and kinetic energies of the coupled beam are

$$\Pi=\Pi_b+\Pi_p==\left(1/2\right)\int_0^L\left\{\begin{array}{c}A_{11}^*u_0'^2-2A_{12}^*u'_0\theta'+A_{22}^*\theta'^2+A_{33}^*\left(w_0'-\theta\right)^2\\-2h_{13}A_pD(u_0'-h\theta'/2)+\beta_{33}^pA_pD^2\end{array}\right\}dx, \tag{13}$$

$$T=T_p+T_p=(1/2)\int_0^L\left\{I_{11}^*\dot{u}_0^2-2I_{12}^*\dot{u}_0\dot{\theta}+I_{22}^*\dot{\theta}^2+I_{11}^*\dot{w}_0^2\right\}dx,$$

where

$$A_{11}^*=A_{11}+C_{11}^pA_p;\ A_{12}^*=A_{12}+C_{11}^pA_ph/2;\ A_{22}^*=A_{22}+C_{11}^p(I_p+A_ph^2/4); \tag{14}$$

$$A_{33}^*=\kappa A_{33}+C_{55}^pA_p;\ I_{11}^*=I_{11}+\rho_pA_p;I_{12}^*=I_{12}+\rho_pA_ph/2;I_{22}^*=I_{22}+\rho_pI_p+\rho_pA_ph^2/4.$$

Putting expressions (13) to the Hamilton's principle

$$\int_{t_1}^{t_2}\delta(T-\Pi)dt=0,$$

one gets

$$\left(I_{11}^*\ddot{u}_0-A_{11}^*u_0''\right)-\left(I_{12}^*\ddot{\theta}-A_{12}^*\theta''\right)+h_{13}A_pD'=0;I_{11}^*\ddot{w}_0-\ A_{33}^*\left(w_0''-\theta'\right)=0;$$

$$\left(I_{12}^*\ddot{u}_0-A_{12}^*u_0''\right)-\left(I_{22}^*\ddot{\theta}-A_{22}^*\theta''\right)+\ A_{33}^*(w_0'-\theta)+h_{13}A_phD'/2=0; \tag{15a}$$

$$h_{13}A_p\left(u_0'-h\theta'/2\right)-\beta_{33}^pA_pD=0$$

and

$$\left[(A_{11}^*u_0'-A_{12}^*\theta'+h_{13}A_pD)\delta u_0\right]_0^L=0;\left[(A_{21}^*u_0'-A_{22}^*\theta'+h_{13}A_phD/2)\delta\theta\right]_0^L=0;$$

$$\left[(A_{33}^*(w_0'-\theta)\delta w_0\right]_0^L=0. \tag{15b}$$

The last equation in (15a) allows one to find $D=h_{13}\left(u_0'-h\theta'/2\right)/\beta_{33}^p$, so that remaining equations in (15) can be written as

$$\left(I_{11}^*\ddot{u}_0-B_{11}^*u_0''\right)-\left(I_{12}^*\ddot{\theta}-B_{12}^*\theta''\right)=0;$$

$$\left(I_{12}^*\ddot{u}_0-B_{12}^*u_0''\right)-\left(I_{22}^*\ddot{\theta}-B_{22}^*\theta''\right)+\ A_{33}^*\left(w_0'-\theta\right)=0; \tag{16}$$

$$I_{11}^*\ddot{w}_0-\ A_{33}^*\left(w_0''-\theta'\right)=0$$

and

$$\left[(B_{11}^*u_0'-B_{12}^*\theta')\delta u_0\right]_0^L=0;\left[(B_{21}^*u_0'-B_{22}^*\theta')\delta\theta\right]_0^L=0;\left[(A_{33}^*(w_0'-\theta)\delta w_0\right]_0^L=0,$$

where the constants

$$B^*_{11},\ B^*_{12},\ B^*_{22}$$

are

$$B^*_{11} = A^*_{11} - A_p h^2_{13}/\beta^p_{33} = A_{11} + E_p A_p,\ \ B^*_{12} = A^*_{12} - A_p h h^2_{13}/2\beta^p_{33} = A_{12} + E_p A_p h/2,$$
$$B^*_{22} = A^*_{22} - A_p h^2 h^2_{13}/4\beta^p_{33} = A_{22} + C^p_{11} I_p + E_p A_p h^2/4;\ \ E_p = C^p_{11} - h^2_{13}/\beta^p_{33}.$$

Transferring equations (16) into the frequency domain, one gets

$$[\mathbf{A}]\{\mathbf{Z}''(x,\omega)\} + [\mathbf{B}]\{\mathbf{Z}'(x,\omega)\} + [\mathbf{C}]\{\mathbf{Z}(x,\omega)\} = 0, \tag{17}$$

where vectors

$$\boldsymbol{Z} = \left\{U(x,\omega), \Theta(x,\omega), W(x,\omega)\right\}^T = \int_{-\infty}^{\infty} \{u_0(x,t), \theta(x,t), w_0(x,t)\} e^{-i\omega t} dt,$$

$$\boldsymbol{Z}' = d\mathbf{Z}/dx, \mathbf{Z}'' = d^2\boldsymbol{z}/dx^2$$

and matrices

$$[\mathbf{A}] = \begin{bmatrix} B^*_{11} & -B^*_{12} & 0 \\ -B^*_{12} & B^*_{22} & 0 \\ 0 & 0 & A^*_{33} \end{bmatrix};\ [\mathbf{B}] = \begin{bmatrix} 0 & 0 & 0 \\ 0 & 0 & A^*_{33} \\ 0 & -A^*_{33} & 0 \end{bmatrix};$$

$$[\mathbf{C}] = \begin{bmatrix} \omega^2 I^*_{11} & -\omega^2 I^*_{12} & 0 \\ -\omega^2 I^*_{12} & \omega^2 I^*_{22} - A^*_{33} & 0 \\ 0 & 0 & \omega^2 I^*_{11} \end{bmatrix}.$$

If the piezoelectric layer is employed as a distributed sensor, the charge output of which can be calculated as

$$Q = \int D dA = b\int_0^L D dx = (bh_{13}/\beta^p_{33})(u_0 - h\theta/2)_0^L. \tag{18}$$

3. Crack model in FGM Timoshenko beam

Assume that the host FGM beam has been cracked at the position e measured from its left end. Recently, some authors, for instance, Aydin (2013); Banerjee, Panigrahi, and Pohit (2016) have proposed to model the crack by a rotational spring of stiffness calculated from the crack depth. Viola, Nobile, and Federici (2002) and Viola, Marzani, and Fantuzzi (2016) and Kim et al. (2018) used two (rotational and transversely extensional) spring model for analysis of cracked homogeneous Timoshenko beam. However, since axial and transverse vibrations in FGM beam are generally coupled, crack could change also axial vibration characteristics. Therefore, crack is modeled in this study by two equivalent springs of stiffness T for axially translational spring and R for rotational one (see Figure 2). Thus, conditions that must be satisfied at the crack are

$$U(e+0) = U(e-0) + N(e)/T\ ;\ \Theta(e+0) = \Theta(e-0) + M(e)/R\ ;\ W(e+0) = W(e-0);$$
$$U'_x(e+0) = U'_x(e-0)\ ;\Theta'_x(e+0) = \Theta'_x(e-0)\ ; W'_x(e+0) = W'_x(e-0) + M(e)/R, \tag{19}$$

where $N(x) = A_{11}U'_x(x); M(x) = A_{22}\Theta'_x(x)$ are respectively internal axial force and bending moment at section x.

Substituting the expressions for axial force and bending moment into (19) that can be rewritten as

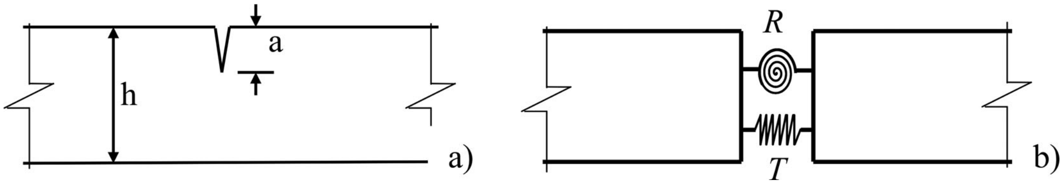

Figure 2. Beam with open edge crack (a) and two spring model of crack (b).

$$U(e+0)=U(e-0)+\gamma_1 U_x'(e)\ ;\ \Theta(e+0)=\Theta(e-0)+\gamma_2\Theta_x'(e)\ ; W(e+0)=W(e-0);$$
$$U_x'(e+0)=U_x'(e-0)\ ;\Theta_x'(e+0)=\Theta_x'(e-0)\ ; W_x'(e+0)=W_x'(e-0)+\gamma_2\Theta_x'(e); \tag{20}$$
$$\gamma_1=A_{11}/T;\gamma_2=A_{22}/R.$$

The so-called crack magnitudes γ_1,γ_2 are functions of the material parameters such as elastic modulus and they should be those of homogeneous beam when $E_t=E_b=E_0$. On the other hand, using expressions (5) the crack magnitudes can be rewritten as

$$\gamma_1=A_{11}/T=\gamma_a\varphi_1(r_e,n)\ ;\gamma_2=A_{22}/R=\gamma_b\varphi_3(r_e,n), \tag{21}$$

where $\gamma_a=E_bA/T;\gamma_b=E_bI_b/R$ and functions $\varphi_1,\ \varphi_3$ defined in (5). In case of homogeneous beam when $r_e=1$ the crack magnitudes would be

$$\gamma_1=\gamma_a\varphi_1(1,0)=\gamma_a=\gamma_{10};,\gamma_2=\gamma_b\varphi_3(1,0)=\gamma_b/12=\gamma_{20},$$

that are calculated from crack depth a for axial and flexural vibrations as (Khiem, Huyen, and Long 2017)

$$\gamma_{10}=E_0A/T=2\pi(1-\nu_0^2)hf_1(z);\ \ \gamma_{20}=E_0I_0/R=6\pi\left(1-\nu_0^2\right)hf_2(z),z=a/h; \tag{22}$$
$$f_1(z)=z^2(0.6272-0.17248z+5.92134z^2-10.7054z^3+31.5685z^4-67.47z^5+$$
$$+139.123z^6-146.682z^7+92.3552z^8);$$
$$f_2(z)=z^2(0.6272-1.04533z+4.5948z^2-9.9736z^3+20.2948z^4-33.0351z^5+$$
$$+47.1063z^6-40.7556z^7+19.6z^8).$$

Thus, for vibration analysis of cracked FGM beam, crack magnitudes are proposed herein to be calculated by

$$\gamma_1=\gamma_{10}\varphi_1(r_e,n)\ ;\gamma_2=12\gamma_{20}\varphi_2(r_3,n). \tag{23}$$

The calculated crack magnitudes γ_1,γ_2 are really dependent on both material and geometrical parameters of FGM beam and they become identical to those of homogeneous beam when $E_t=E_b=E_0$ or $r_e=1$.

4. General solution for free vibration of cracked FGM beam with piezoelectric layer

Seeking solutions of equation (17) in the form: $\boldsymbol{Z}_0=\boldsymbol{d}e^{\lambda x}$ leads to characteristic equation

$$\det[\lambda^2\mathbf{A}+\lambda\mathbf{B}+\mathbf{C}]=0 \tag{24}$$

This is in fact a cube algebraic equation with respect to $\eta=\lambda^2$ that can be easily solved to give three roots η_1,η_2,η_3, so that one obtains $\lambda_{1,4}=\pm k_1;\lambda_{2,5}=\pm k_2;\lambda_{3,6}=\pm k_3;k_j=\sqrt{\eta_j},j=1,2,3$. Consequently, general solution of equation (17) is represented as

$$\{\mathbf{Z}_0\} = \begin{bmatrix} d_{11} & d_{12} & \dots & d_{16} \\ d_{21} & d_{22} & \dots & d_{26} \\ d_{31} & d_{32} & \dots & d_{36} \end{bmatrix} \cdot \begin{Bmatrix} e^{\lambda_1 x} \\ \vdots \\ e^{\lambda_6 x} \end{Bmatrix} = \begin{bmatrix} \alpha_1 C_1 & \alpha_2 C_2 & \dots & \alpha_6 C_6 \\ C_1 & C_2 & \dots & C_6 \\ \beta_1 C_1 & \beta_2 C_2 & \dots & \beta_6 C_6 \end{bmatrix} \cdot \begin{Bmatrix} e^{\lambda_1 x} \\ \vdots \\ e^{\lambda_6 x} \end{Bmatrix}$$

with constants $C_1, \dots, C_6$ and

$$\alpha_j = (\omega^2 I_{11}^* + \eta_j B_{11}^*)/(\omega^2 I_{12}^* + \eta_j B_{12}^*); \beta_j = \lambda_j \ A_{33}^*/\left(\omega^2 I_{11}^* + \eta_j \ A_{33}^*\right); \ j = 1, 2, 3.$$

The latter expressions show that $\alpha_4 = \alpha_1; \alpha_5 = \alpha_2; \alpha_6 = \alpha_3; \beta_4 = -\beta_1; \beta_5 = -\beta_2; \beta_6 = -\beta_3$. Therefore, general solution of (17) can be rewritten in the form

$$\{\mathbf{Z}_0(x, \omega)\} = [\mathbf{G}_0(x, \omega)]\{\mathbf{C}\} \tag{25}$$

where $\{\mathbf{C}\} = (C_1, \dots, C_6)^T$ and $\mathbf{G}_0(x, \omega)$ is

$$[G_0(x, \omega)] = \begin{bmatrix} \alpha_1 e^{k_1 x} & \alpha_2 e^{k_2 x} & \alpha_3 e^{k_3 x} & \alpha_1 e^{-k_1 x} & \alpha_2 e^{-k_2 x} & \alpha_3 e^{-k_3 x} \\ e^{k_1 x} & e^{k_2 x} & e^{k_3 x} & e^{-k_1 x} & e^{-k_2 x} & e^{-k_3 x} \\ \beta_1 e^{k_1 x} & \beta_2 e^{k_2 x} & \beta_3 e^{k_3 x} & -\beta_1 e^{-k_1 x} & -\beta_2 e^{-k_2 x} & -\beta_3 e^{-k_3 x} \end{bmatrix} \tag{26}$$

Now, we seek a particular solution $\mathbf{Z}_c(x, \omega)$ of Eq. (17) that satisfies the conditions

$$\{\mathbf{Z}_c(0)\} = \left(\gamma_a U_0'(e), \gamma_b \Theta_0'(e), 0\right)^T; \left\{\mathbf{Z}_c'(0)\right\} = \left(0, 0, \gamma_b \Theta_0'(e)\right)^T \tag{27}$$

Putting expression (25) into (27) one finds

$$\{\mathbf{Z}_c(x, \omega)\} = [\mathbf{G}_c(x, \omega)]\left\{\mathbf{Z}_0'(e, \omega)\right\} \tag{28}$$

where $\mathbf{G}(x, \omega)$ is 3×3-matrix of the form

$$[\mathbf{G}_c(x, \omega)] = \begin{bmatrix} \gamma_a \sum_{i=1}^3 \alpha_i \delta_{i1} \cos hk_i x & \gamma_b \sum_{i=1}^3 \alpha_i (\delta_{i2} + \delta_{i3}) \cos hk_i x & 0 \\ \gamma_a \sum_{i=1}^3 \delta_{i1} \cos hk_i x & \gamma_b \sum_{i=1}^3 (\delta_{i2} + \delta_{i3}) \cos hk_i x & 0 \\ \gamma_a \sum_{i=1}^3 \beta_i \delta_{i1} \sin hk_i x & \gamma_b \sum_{i=1}^3 \beta_i (\delta_{i2} + \delta_{i3}) \sin hk_2 x & 0 \end{bmatrix} \tag{29}$$

and

$$\delta_{11} = (k_3\beta_3 - k_2\beta_2)/\Delta; \delta_{12} = (\alpha_3 k_2 \beta_2 - \alpha_2 k_3 \beta_3)/\Delta; \delta_{13} = (\alpha_2 - \alpha_3)/\Delta;$$

$$\delta_{21} = (k_1\beta_1 - k_3\beta_3)/\Delta; \delta_{22} = (\alpha_1 k_3 \beta_3 - \alpha_3 k_1 \beta_1)/\Delta; \delta_{23} = (\alpha_3 - \alpha_1)/\Delta;$$

$$\delta_{31} = (k_2\beta_2 - k_1\beta_1)/\Delta; \delta_{32} = (\alpha_2 k_1 \beta_1 - \alpha_1 k_2 \beta_2)/\Delta; \delta_{33} = (\alpha_1 - \alpha_2)/\Delta;$$

$$\Delta = k_1\beta_1(\alpha_2 - \alpha_3) + k_2\beta_2(\alpha_3 - \alpha_1) + k_3\beta_3(\alpha_1 - \alpha_2).$$

Therefore, it is easily to verify that solution of Eq. (17) satisfying the conditions (20) can be represented as

$$\{\mathbf{Z}(x, \omega)\} = \begin{cases} \{\mathbf{Z}_0(x, \omega)\} : \text{for } x < e \\ \{\mathbf{Z}_0(x, \omega)\} + \{\mathbf{Z}_c(x - e, \omega)\} : \text{for } e \le x \end{cases}$$

that is rewritten in the form

$$\{\mathbf{Z}(x, \omega)\} = \{\mathbf{Z}_0(x, \omega)\} + [\mathbf{K}(x - e)] \cdot \left\{\mathbf{Z}_0'(e, \omega)\right\} = [\mathbf{\Phi}(x, \omega)]\{\mathbf{C}\}, \tag{30}$$

with the matrices introduced

$$[\mathbf{\Phi}(x, \omega)] = \left[\mathbf{G}_0(x, \omega) + \mathbf{K}(x - e)\mathbf{G}_0'(x, \omega)\right]; \tag{31}$$

$$[\mathbf{K}(x)] = \begin{cases} [\mathbf{G}_c(x)] & : x > 0; \\ [0] : & x \le 0; \end{cases} \quad [\mathbf{K}'(x)] = \begin{cases} [\mathbf{G}_c'(x)] & : x > 0; \\ [0] : & x \le 0. \end{cases}$$

By similar way one can obtain general solution for free vibration of the beam with multiple cracks in the form (30) with

$$[\mathbf{\Phi}(x,\omega)] = [\mathbf{G}_0(x,\omega)] + \sum_{j=1}^{n} [\mathbf{K}(x-e_j)] \cdot [\mathbf{M}_j]; \;\; [\mathbf{M}_j] = [\mathbf{G}_0'(e_j,\omega)] + \sum_{k=1}^{j-1} [\mathbf{G}'(e_j - e_k)] \cdot [\mathbf{M}_k].$$

Thus, expression (30) is general solution for free vibration of cracked FGM beam with piezoelectric layer, that will be used for free vibration analysis of the beam in different cases of boundary conditions as following. Namely, for simply supported beam with boundary conditions

$$U(0) = W(0) = M(0) = U(L) = W(L) = M(L) = 0$$

with $M(x) = B_{12}^* \partial_x U(x) - B_{22}^* \partial_x \Theta(\mathrm{x}),$ one gets

$$[\mathbf{B}(\omega)]\{C\} = 0, \tag{32}$$

where

$$[\mathbf{B}(\omega)] = [\mathbf{B}_{SS}(\omega)] = \begin{bmatrix} \alpha_1 & \alpha_2 & \alpha_3 & \alpha_1 & \alpha_2 & \alpha_3 \\ \beta_1 & \beta_2 & \beta_3 & -\beta_1 & -\beta_2 & -\beta_3 \\ m_1 & m_2 & m_3 & -m_1 & -m_2 & -m_3 \\ \phi_{11}(L) & \phi_{12}(L) & \phi_{13}(L) & \phi_{14}(L) & \phi_{15}(L) & \phi_{16}(L) \\ \phi_{31}(L) & \phi_{32}(L) & \phi_{33}(L) & \phi_{34}(L) & \phi_{35}(L) & \phi_{36}(L) \\ M_1(L) & M_2(L) & M_3(L) & M_4(L) & M_5(L) & M_6(L) \end{bmatrix}$$

$$m_j = (B_{12}^* \alpha_j - B_{22}^*) k_j, \;\; j = 1,2,3; \;\; M_j(L) = B_{12}^* \phi_{1j}'(L) - B_{22}^* \phi_{2j}'(L), j = 1,2,...,6;$$

$\phi_{ij}(x), \phi_{ij}'(x),\;\; i = 1,2,3; j = 1,2,....,6$ are elements of matrices $[\mathbf{\Phi}(x,\omega)]$ and $[\mathbf{\Phi}'(x,\omega)]$ defined in (31). Therefore, frequency equation of the beam is

$$\det[\mathbf{B}(\omega)] = 0,$$

positive roots of which give rise desired natural frequencies $\omega_1, \omega_2, \omega_3,$ .... of simply supported FGM beam with piezoelectric layer and cracks. For every given natural frequency ω_k, a normalized of solution of Eq. (32) can be easily found as $(\vartheta_1, ..., \vartheta_6)$ that allow one to calculate corresponding mode shape in the form

$$\begin{aligned} U_k(x) &= C_k\left(\alpha_1 \vartheta_1 e^{k_1 x} + \alpha_2 \vartheta_2 e^{k_2 x} + \alpha_3 \vartheta_3 e^{k_3 x} + \alpha_1 \vartheta_4 e^{-k_1 x} + \alpha_2 \vartheta_5 e^{-k_2 x} + \alpha_3 \vartheta_6 e^{-k_3 x}\right); \\ \Theta_k(x) &= C_k\left(\vartheta_1 e^{k_1 x} + \vartheta_2 e^{k_2 x} + \vartheta_3 e^{k_3 x} + \vartheta_4 e^{-k_1 x} + \vartheta_5 e^{-k_2 x} + \vartheta_6 e^{-k_3 x}\right); \\ W_k(x) &= C_k\left(\beta_1 \vartheta_1 e^{k_1 x} + \beta_2 \vartheta_2 e^{k_2 x} + \beta_3 \vartheta_3 e^{k_3 x} - \beta_1 \vartheta_4 e^{-k_1 x} - \beta_2 \vartheta_5 e^{-k_2 x} - \beta_3 \vartheta_6 e^{-k_3 x}\right), \end{aligned} \tag{33}$$

where arbitrary constant C_k can be obtained from a chosen mode shape normalization, for instance,

$$\max_x |W_k(x)| = 1.$$

Using the mode shape, it can be calculated so-called hereby modal sensor output (MSO) charge generated in the piezoelectric layer as

$$Q_k = (bh_{13}/\beta_{33}^p) \int_0^L \left[U_k'(x) - h\Theta_k'(x)/2\right] dx =$$

Table 1. Frequency parameter $\lambda = \omega(L^2/h)\sqrt{\rho_b/E_b}$ of SS-beam for various thickness of piezoelectric layer and slenderness ratio L_b/h_b with material gradient index $n = 2$.

		Thickness ratio (h_p/h_b)							
L/h	S&B[1]	0	0.1	0.2	0.3	0.5	0.8	1.0	Mode no.
5	3.390	3.3309	3.2692	3.2562	3.2825	3.4193	3.7344	3.9644	1
	11.740	11.5403	11.1982	10.9848	10.8701	10.8345	10.9677	10.9426	2
	19.479	19.3733	18.6362	17.9243	17.2200	15.8054	13.7393	12.6102	3
	22.387	22.0386	21.2443	20.6727	20.2772	19.8542	19.6831	19.3017	4
	33.912	33.4451	32.1182	31.1010	30.3348	28.3738	22.3316	20.0871	5
10	3.551	3.4878	3.4391	3.4463	3.5005	3.7159	4.2049	4.5837	1
	13.561	13.3229	13.0637	12.9806	13.0362	13.4377	14.4093	15.1185	2
	28.544	28.0555	27.3652	27.0203	26.9446	27.3438	28.6153	27.9506	3
	38.958	**38.9090**	**37.2752**	**35.8374**	**34.5478**	**32.3022**	**29.5240**	**29.5703**	4
	46.941	46.1729	44.8284	44.0161	43.6156	43.6458	44.6972	45.5729	5
20	3.5957	3.5315	3.4870	3.5010	3.5643	3.8073	4.3637	4.8077	1
	14.202	13.9511	13.7439	13.7372	13.8932	14.5677	16.1230	17.3268	2
	31.319	30.7718	30.2546	30.1695	30.4323	31.7158	34.7137	36.9909	3
	54.220	53.2913	52.2522	51.9119	52.1163	53.6065	56.2525	55.7982	4
	77.917	77.9014	74.5954	71.7766	69.3396	65.3857	62.0291	62.9888	5
30	3.6042	3.5398	3.4962	3.5114	3.5767	3.8252	4.3958	4.8541	1
	14.334	14.0799	13.8853	13.8968	14.0772	14.8205	16.5357	17.8880	2
	31.950	31.3899	30.9273	30.9222	31.2908	32.8653	36.5016	39.3333	3
	56.077	55.1111	54.2191	54.0984	54.5976	56.9407	62.3101	66.2509	4
	86.244	84.7885	83.2903	82.9572	83.5559	86.7580	90.9312	87.5998	5

[1]Su and Banerjee 2015.

$$= (bh_{13}/\beta_{33}^p)\left\{\int_0^e \left[U_k'(x) - h\Theta_k'(x)/2\right]dx + \int_e^L \left[U_k'(x) - h\Theta_k'(x)/2\right]dx\right\} =$$

$$= (bh_{13}/\beta_{33}^p)\left\{\left[U_k(L) - U_k(0) - \gamma_1 U_x'(e)\right] - \left(h/2\right)\left[\Theta_k(L) - \Theta_k(0) - \gamma_2\Theta_x'(e)\right]\right\}, \quad (34)$$

where γ_1, γ_2 are crack magnitudes defined above in Eq. (23). This modal sensor output will be numerically examined below mutually with natural frequencies and mode shapes of FGM beam with piezoelectric layer in dependence of crack location and depth.

4. Numerical results and validation

Consider an FGM beam bonded by a piezoelectric layer as shown in Figure 1 with the following properties

$$L_b = L_p = L = 1\text{m}; b = 0.1\text{m}; \ \ h_b = L/10;$$

$$E_t = 390\text{MPa}, \ \ \rho_t = 3960\text{kg/m}^3, \ \ \mu_t = 0.25; E_b = 210\text{MPa}, \ \ \rho_b = 7800\text{kg/m}^3, \mu_t = 0.31;$$

$$C_{11}^p = 69.0084\text{GPa}, \ \ C_{55}^p = 21.0526\text{GPa}, \ \ \rho_p = 7750\text{kg/m}^3, h_{13} = -7.70394\times 10^8 V/m.$$

First, natural frequency parameters $\lambda_k = \omega_k(L^2/h)\sqrt{\rho_b/E_b}$, $k = 1, 2, ..., 5$ are computed for relative thickness of piezoelectric layer h_p/h_b varying from 0 to 1 in various slenderness ratio L_b/h_b and material grading index n.

The dimensionless natural frequencies obtained for simply supported intact beam are shown in Tables 1 and 2 where the frequencies given in Su and Banerjee 2015 for FGM beam without piezoelectric layer are also presented. Comparing the latter results with those obtained in the present study with $h_p = 0$ shows a good agreement. Furthermore, variation of the natural frequencies versus piezoelectric layer thickness observed in the Tables 1 and 2 demonstrates exactly the fact that was found in Khiem, Hai and Huong (2020) such as: natural frequencies of FGM beam are first decreasing then increasing with growing thickness of piezoelectric layer. So, the

Table 2. Frequency parameter $\lambda = \omega(L^2/h)\sqrt{\rho_b/E_b}$ of SS-beam for various thickness of piezoelectric layer and material gradient index (n) with slenderness ratio $L_b/h_b = 10$.

		Thickness ratio (h_p/h_b)							
n	S&B[1]	0	0.1	0.2	0.3	0.5	0.8	1.0	Mode no.
0.1	5.0001	4.9977	4.7446	4.5982	4.5326	4.5757	4.9095	5.2269	1
	19.136	19.1228	18.0545	17.3675	16.9592	16.7134	17.1478	17.6743	2
	40.385	40.3570	37.8771	36.1858	35.0671	33.9903	33.9840	34.3554	3
	56.379	56.3731	52.3509	49.0886	46.3555	41.9528	36.9877	34.4557	4
	66.608	66.5611	62.1356	58.9890	56.7733	54.2305	53.0524	53.0788	5
0.2	4.7348	4.7243	4.5141	4.3987	4.3567	4.4333	4.7976	5.1276	1
	18.118	18.0772	17.1789	16.6146	16.2991	16.1827	16.7297	17.2997	2
	38.240	38.1525	36.0483	34.6295	33.7175	32.9303	33.1794	33.5028	3
	53.361	53.5455	50.0038	47.0891	44.6188	40.5881	35.9746	33.7527	4
	63.075	62.9317	59.1515	56.4747	54.6155	52.5701	51.8254	52.0219	5
0.5	4.2432	4.2086	4.0718	4.0114	4.0120	4.1502	4.5708	4.9240	1
	16.235	16.1021	15.4951	15.1474	14.9984	15.1171	15.8680	16.5140	2
	34.261	33.9801	32.5199	31.5828	31.0435	30.7871	31.5069	31.6420	3
	48.044	48.0050	45.2957	43.0046	41.0196	37.6991	33.7845	32.2653	4
	56.502	56.0479	53.3753	51.5314	50.3178	49.1901	49.2525	49.7644	5
1.0	3.8586	3.8004	3.7156	3.6950	3.7271	3.9111	4.3732	4.7427	1
	14.755	14.5331	14.1315	13.9400	13.9126	14.2022	15.0944	15.7871	2
	31.110	30.6491	29.6432	29.0550	28.7896	28.9250	29.9851	29.7951	3
	43.242	43.1884	41.0914	39.2787	37.6791	34.9455	31.6388	30.8712	4
	51.256	50.5213	48.6317	47.3940	46.6587	46.2166	46.8768	47.6156	5
2.0	3.551	3.4878	3.4391	3.4463	3.5005	3.7159	4.2049	4.5837	1
	13.561	13.3229	13.0637	12.9806	13.0362	13.4377	14.4093	15.1185	2
	28.544	28.0555	27.3652	27.0203	26.9446	27.3438	28.6153	27.9506	3
	38.958	38.9090	37.2755	35.8374	34.5478	32.3022	29.5240	29.5703	4
	46.941	46.1729	44.8284	44.0161	43.6156	43.6458	44.6972	45.5729	5
5.0	3.2608	3.2251	3.2037	3.2323	3.3034	3.5427	4.0507	4.4350	1
	12.434	12.3013	12.1500	12.1489	12.2665	12.7468	13.7614	14.4681	2
	26.122	25.8533	25.4021	25.2422	25.3092	25.9001	27.3075	26.0857	3
	35.052	35.0281	33.7532	32.6122	31.5740	29.7346	27.4146	28.2954	4
	42.873	42.4555	41.5224	41.0330	40.8855	41.2645	42.5836	43.5408	5
10	3.0959	3.0805	3.0730	3.1133	3.1941	3.4484	3.9696	4.3584	1
	11.805	11.7476	11.6514	11.6949	11.8481	12.3778	13.4266	14.1381	2
	24.799	24.6834	24.3531	24.2919	24.4391	25.1448	26.4425	25.2175	3
	33.371	33.3619	32.2232	31.1959	30.2547	28.5752	26.6432	27.6582	4
	40.700	40.5218	39.7921	39.4708	39.4610	40.0391	41.5217	42.5328	5

[1]Su and Banerjee 2015.

agreement of the results obtained in this study for the case of uncracked FGM beam compared to the earlier published ones is adequate to validate the above proposed theoretical development.

4.1. Natural frequencies and mode shapes of cracked FGM beam with piezoelectric layer

As one of the fundamental dynamic characteristics of a structure, natural frequencies represent both the structure stiffness and mass distribution and any change in stiffness or mass of an elastic structure is vitally leading to variation of natural frequencies. Therefore, natural frequencies have been acknowledged as an efficient indicator for structural health monitoring, especially, in structural damage detection using the nondestructive technique. In the structural damage detection such as crack identification using the natural frequency-based method, measurements of natural frequencies are usually performed by using the conventional modal testing technique. While, the lumped sensors often reduce structure natural frequencies, the distributed piezoelectric sensors may also increase the natural frequencies in dependence upon size of the sensors. So, effect of distributed piezoelectric sensors on natural frequencies of cracked structures is important information for the structural crack detection from measured natural frequencies. Effect of piezoelectric patch on natural frequencies of undamaged FGM beam were studied in Khiem, Hai and

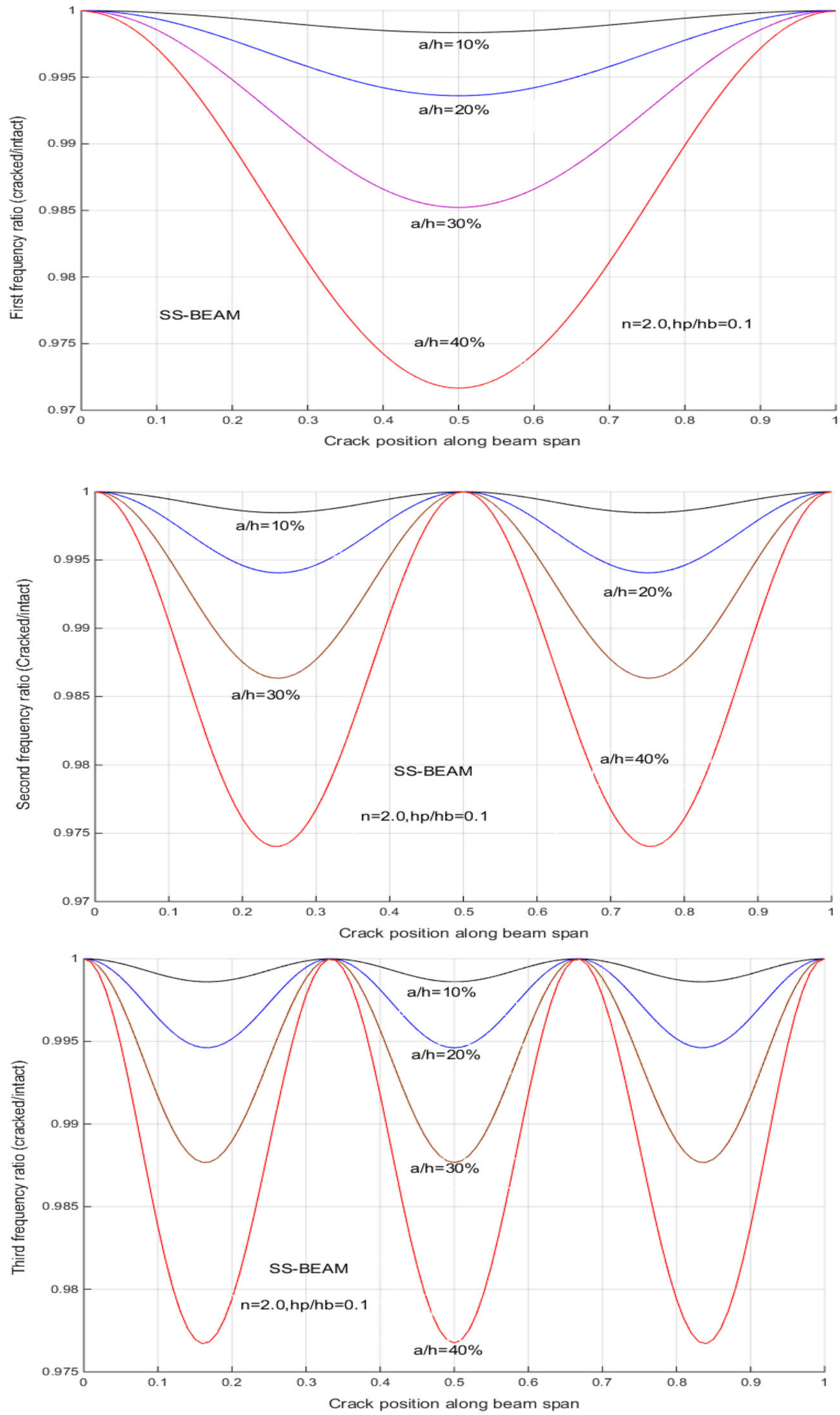

Figure 3. Variation of first three natural frequencies caused by crack position and depth.

Huong (2020), in the present subsection the crack-induced variations, usually treated as sensitivity to crack, of natural frequencies are examined for FGM beam with piezoelectric layer. Namely, the ratio of natural frequencies of cracked beam to those of intact one is computed as function of crack position along the beam span for various crack depth (a/h), material gradient index (n) and

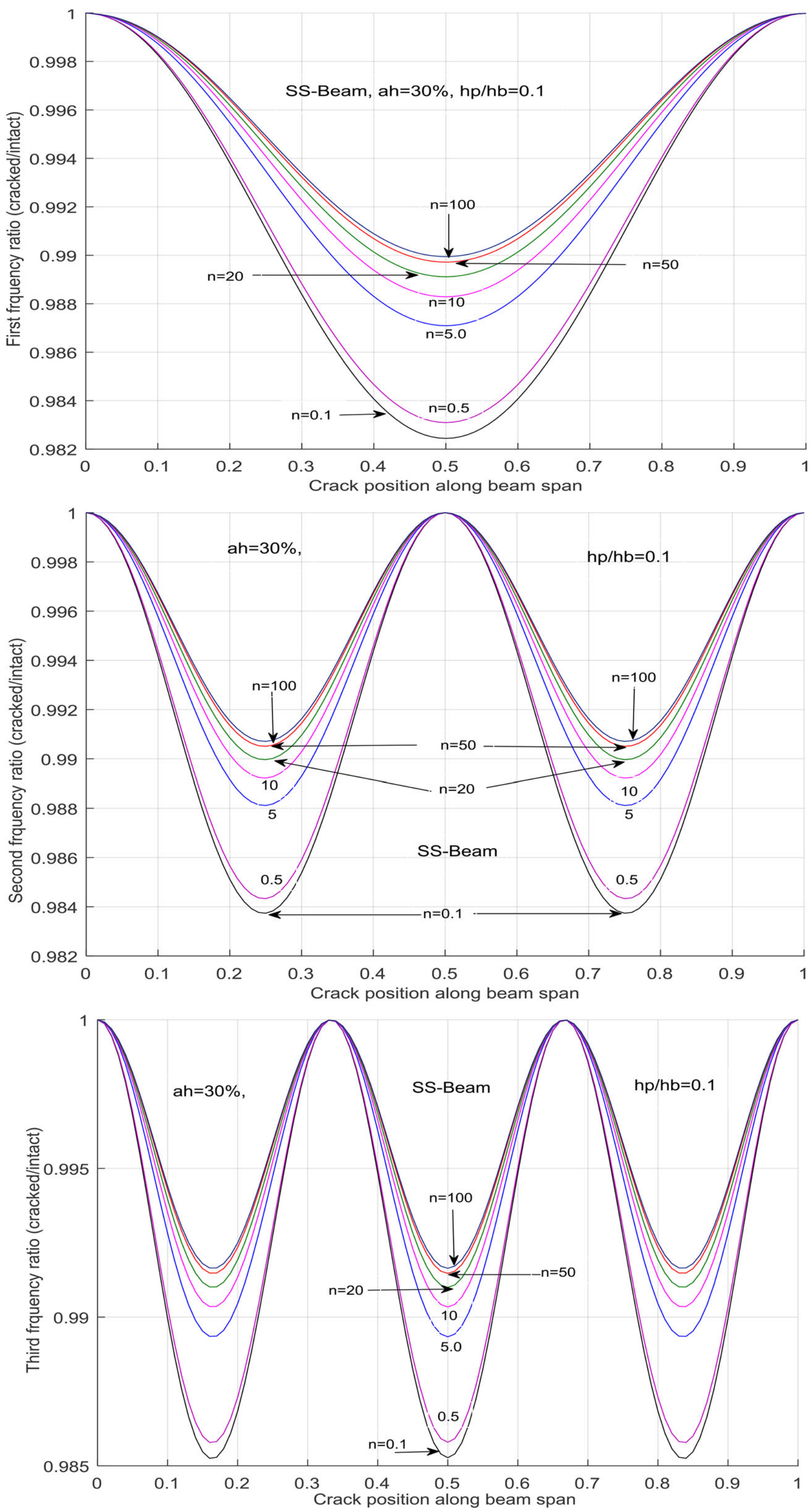

Figure 4. Variation of first three natural frequencies versus crack position in various material gradient index *n*.

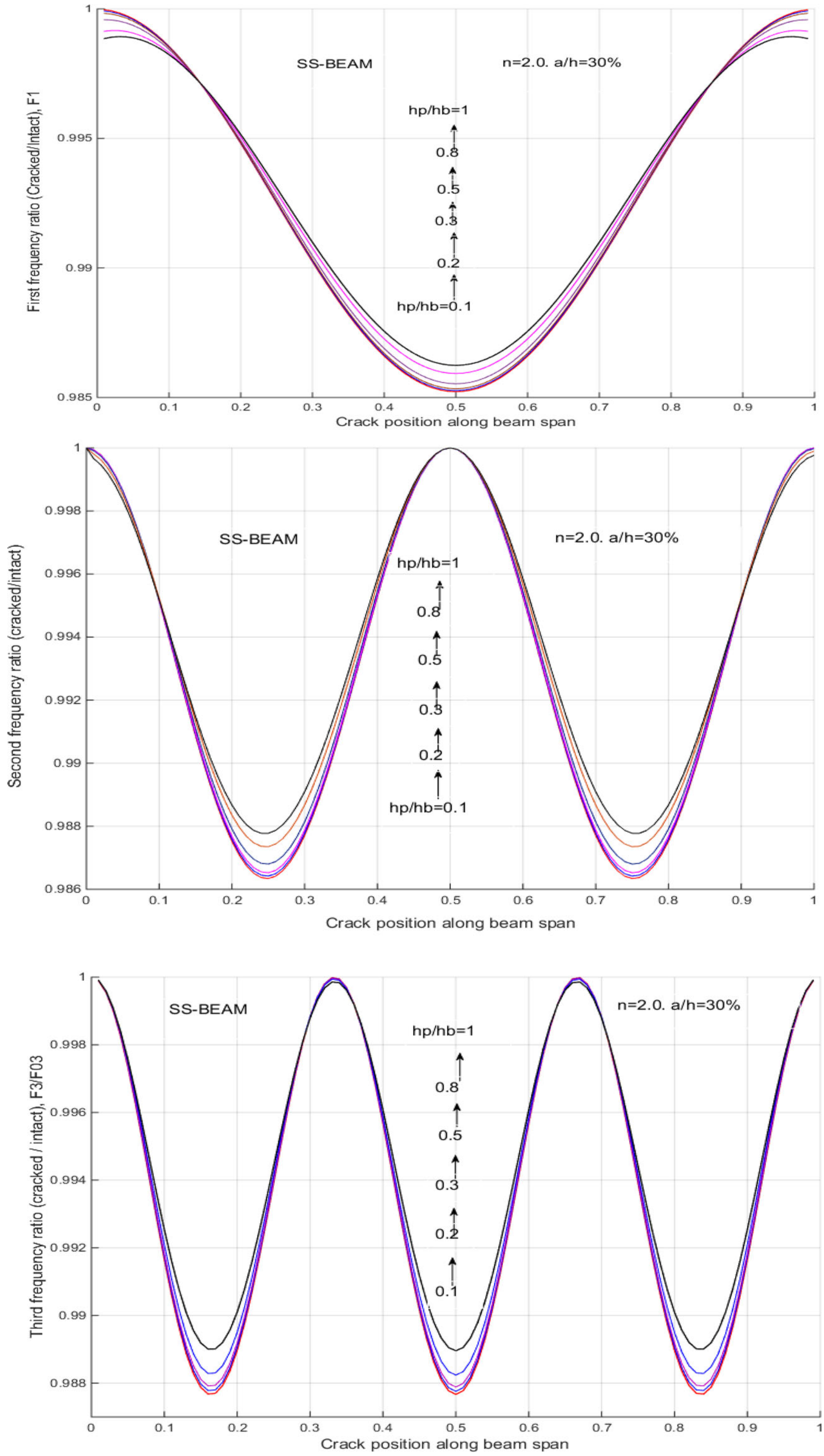

Figure 5. Variation of first three natural frequencies versus crack position in various thickness of piezoelectric layer.

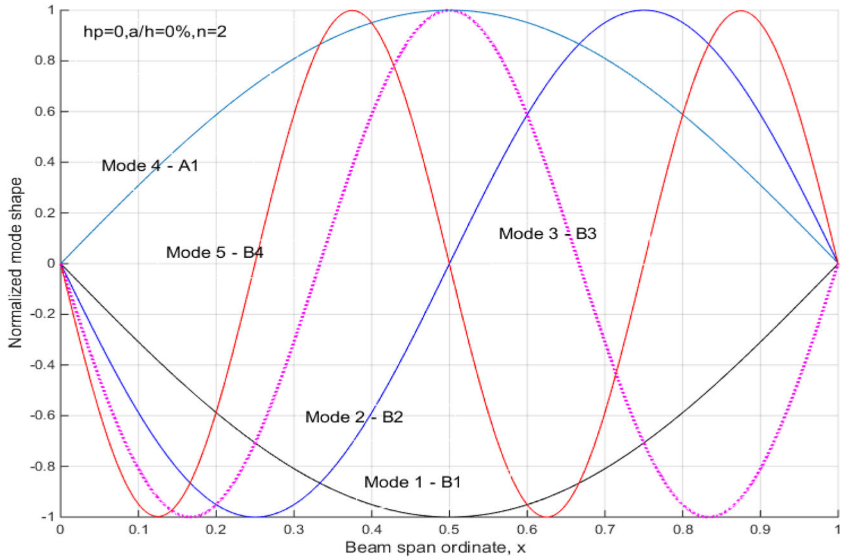

Figure 6. Five lowest mode shapes of uncracked beam without piezoelectric layer.
(A1 – first axial vibration mode; B1-B4 – Lowest four flexural vibration modes)

piezoelectric layer (h_p/h_b). The ratios or dimensionless frequencies of three lowest modes obtained for simply supported (SS-) beam are shown in Figures 3–5. It can be observed from the Figures that natural frequency sensitivity to crack position and depth (Figure 3) for FGM beam with piezoelectric layer is similar to that of homogeneous beam or FGM beam (Khiem, Huyen, and Long 2017) without piezoelectric layer. The increasing material gradient index n reduces the natural frequency sensitivity to crack independently upon presence of the piezoelectric layer (Figure 4).

Graphics presented in Figure 5 show that thickness of the piezoelectric layer is less affecting the natural frequency sensitivity to crack in comparison with the crack depth and material gradient index, it may slightly reduce the sensitivity in vicinity of the positions on beam where natural frequencies are most sensitive to crack. Mode shapes of five natural mode shapes were computed for uncracked FGM beam without piezoelectric layer and cracked FGM beam with piezoelectric layer and are presented in Figures 6 and 7. Comparison of the obtained mode shapes allows one to conclude that material grading, presence of crack and piezoelectric layer do not change mode shapes of the beam.

4.2. Modal sensor charge of piezoelectric layer bonded to cracked FGM beam

Likely to that carried out above, in this subsection, crack-induced variations of the so-called modal sensor charge determined by expression (30) for lowest natural modes of simply supported beam are numerically examined in dependence upon crack parameters, material gradient index and piezoelectric layer thickness. First, the modal sensor outputs are computed as function of crack position for various crack depth and results of computation are depicted in Figure 8. It is observed insignificant sensor output charge for the second natural mode compared to the first and third modes, especially, in case of uncracked beam and the charge is very slightly altered due to crack appeared to the beam. This may be caused by two facts: (1) the sensor has the same length as the beam and (2) boundary conditions of the beam are symmetric. Moreover, it is noteworthy that there are exist positions on beam, crack appeared at which makes no effect on the modal charge. Such critical positions on beam can be also called node of modal sensor charge likely that of natural frequencies. It can be exactly observed (k-1) nodes for sensor output of k-th

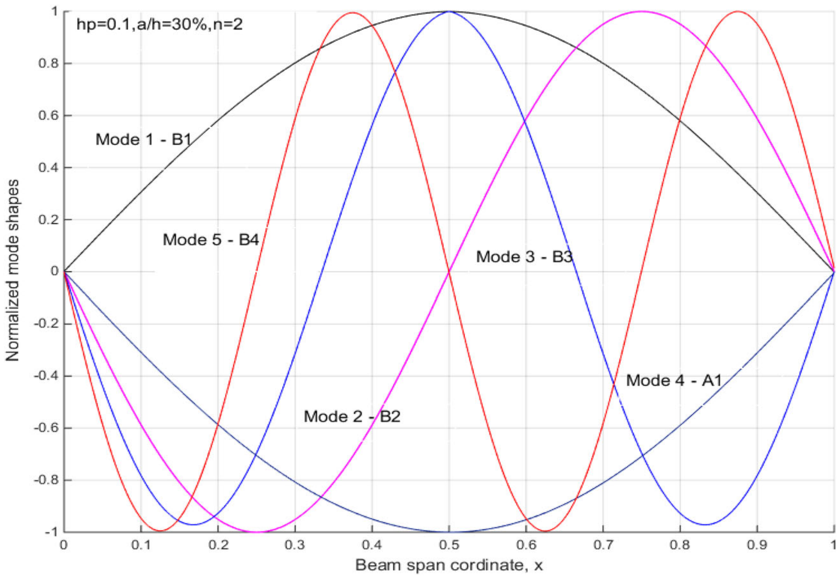

Figure 7. Five lowest mode shapes of cracked beam with piezoelectric layer.
(A1 – first axial vibration mode; B1-B4 – Lowest four flexural vibration modes)

mode like those of mode shapes itself (see Figures 6 and 7). The observed nodes of third sensor outputs demonstrate the fact that crack appeared between the nodes reduces the output charge of full-length piezoelectric sensor and crack appeared outside the node segment increases the output charge. This is an efficient indicator or crack localization by using modal sensor charge. Observation of the graphs given the Figures 9 and 10 reveals a fact that decreasing material gradient index and increasing thickness of piezoelectric layer both lead to amplify the modal sensor outputs. Moreover, asymmetry of graphics representing variation of sensor output charge gets to be stronger with increasing thickness of piezoelectric layer (Figure 10). This can be explained by the fact that since the charge is calculated from both axial and bending vibration mode shapes, as shown in Eq. (34), its variation must be dependent upon the mode shapes, their derivatives and the interaction between the vibration modes. The different variation of axial and flexural vibration characteristics should lead to complicate variation of the charge.

5. Conclusions

Thus, in the present study, there is conducted a model of cracked FGM beam bonded full-length with piezoelectric layer based on the Timoshenko beam theory, power law of material grading and double spring model of open transverse crack. The established governing equations of the smart FGM beam show that piezoelectric layer bonded to a beam makes an important contribution to the coupling of axial and flexural vibration modes. So that axial vibration modes may have an effect on either mechanical or electrical behavior of the coupled beam structure.

There has been obtained general solution for free vibration of the coupled beam with crack that allows fruitfully computing not only the modal parameters such as natural frequencies and mode shapes of the beam structure but also the output charge under natural vibration modes called herein modal sensor charge of piezoelectric layer. Moreover, an expression of the modal sensor charges was obtained explicitly with respect to the crack parameters that provides a useful tool for crack detection from measured modal sensor charges.

The normalized natural frequencies and modal sensor outputs (the ratios of cracked to intact) have been thoroughly examined as function of crack position (called herein crack-induced

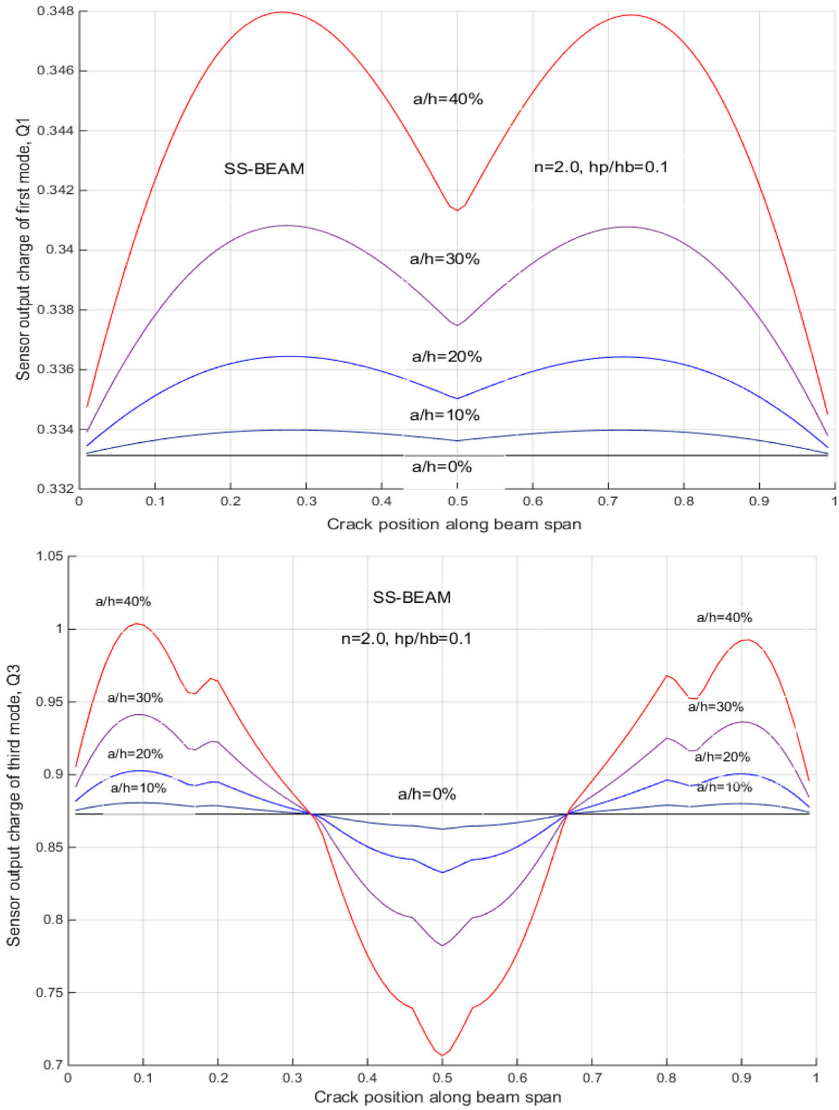

Figure 8. Crack-induced variation of modal sensor charge of first and third modes in various crack depth.

variation) in dependence on crack depth, material gradient index and thickness of the piezoelectric layer. The completed modal analysis enables to make following concluding remarks:

1. Variation of natural frequencies is growing with increasing crack depth, decreasing material gradient index and thickness of piezoelectric layer.
2. Modal sensor charge is amplified by decreasing material gradient index and increasing thickness of piezoelectric layer, but crack depth may increase or decrease the modal sensor charge in dependence on where the crack is located.
3. There exist positions on the beam, crack appeared at which does not change both natural frequency and modal sensor charge of a certain mode that are called nodes of the natural frequency and modal sensor charge.

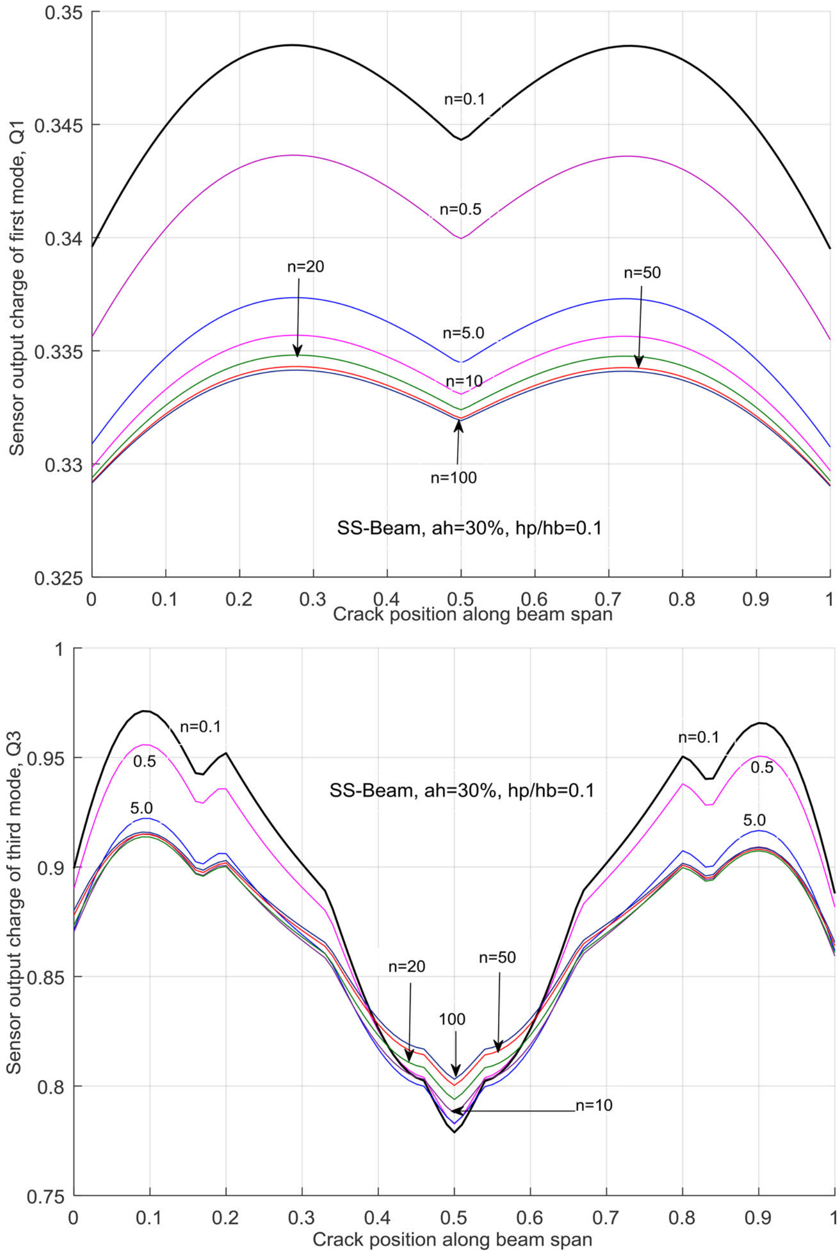

Figure 9. Crack-induced variation of modal sensor charge of first and third modes in various material gradient index *n*.

4. Both material gradient index and piezoelectric layer thickness make no effect on natural mode shapes of the beam and insignificant charge generated in the full-length piezoelectric sensor due to natural vibration of second mode in simply supported beam.

Similar analysis could be carried out for beam with other boundary conditions and the obtained results mentioned above can be efficiently used for solving the crack detection in FGM beam by using piezoelectric sensors. Especially, measuring the sensor output charge is more easily than modal parameters such as natural frequencies and mode shapes or even than EMI measurements. Hence, the analysis of modal sensor charge in dependence on crack parameters completed

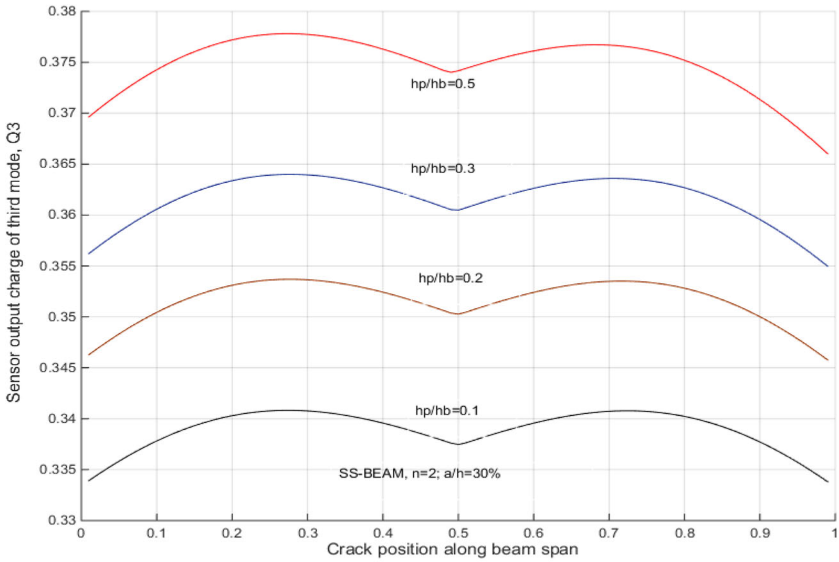

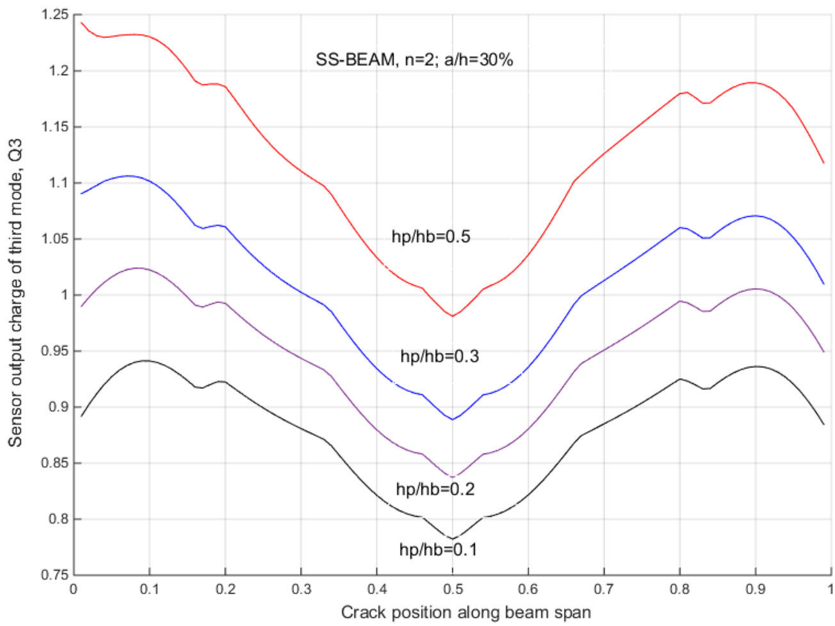

Figure 10. Crack-induced variation of modal sensor charge of first and third modes in various thickness of piezoelectric layer.

in this study is the essential step to use smart sensor for structural health monitoring of composite structures in the practice. Nevertheless, the results obtained in this study are limited to apply for beam-like structures such as stepped and multispan beams or frame that is composed from beam elements. In the case the dynamic stiffness method should be applied for assembling all the beam elements with piezoelectric layer. It might be used for health monitoring only that large machinery or equipment with beam elements.

Funding

This research was funded by National Foundation for Science and Technology Development (NAFOSTED) of Vietnam under Project number 107.01-2019.312.

ORCID

Nguyen Tien Khiem http://orcid.org/0000-0001-5195-2704

References

Akbas, S. D. 2013. Free vibration characteristics of edge cracked functionally graded beams by using finite element method. *International Journal of Engineering Trends and Technology* 4 (10):4590–7.

Aydin, K. 2013. Free vibration of functionally graded beams with arbitrary number of surface cracks. *European Journal of Mechanics - A/Solids* 42:112–24. doi: 10.1016/j.euromechsol.2013.05.002.

Banerjee, A., B. Panigrahi, and G. Pohit. 2016. Crack modelling and detection in Timoshenko FGM beam under transverse vibration using frequency contour and response surface model with GA. *Nondestructive Testing and Evaluation* 31 (2):142–64. doi: 10.1080/10589759.2015.1071812.

Bendine, K., F. B. Boukhoulda, M. Nouari, and Z. Satla. 2016. Active vibration control of functionally graded beams with piezoelectric layers based on higher order shear deformation theory. *Earthquake Engineering and Engineering Vibration* 15 (4):611–20. doi: 10.1007/s11803-016-0352-y.

Bhalla, S., and C.-K. Soh. 2006. Progress in structural health monitoring and non-destructive evaluation using piezo-impedance transducers. In: *Smart material and structures: new research*, ed. P. L. Reece, Chapter 6, 177–228. New York: Nova Science Publisher, Inc.

Crawley, E. F., and J. De Luis. 1987. Use of piezoelectric actuators as elements of intelligent structures. *AIAA Journal* 25 (10):1373–85. doi: 10.2514/3.9792.

Duan, W. H., Q. Wang, and S. T. Quek. 2010. Application of piezoelectric material in structural health monitoring and repair: selected research examples. *Materials (Basel, Switzerland)* 3 (12):5169–94. doi: 10.3390/ma3125169.

Fan, W., and P. Z. Qiao. 2011. Vibration-based damage identification methods: A review and comparative study. *Struct. Health Monit* 10 (1):83–111.

Giurgiutiu, V. 2007. *Structural health monitoring with piezoelectric wafer active sensors*, 747. Oxford: Academic Press

Golewski, G. L. 2021. The Beneficial effect of the addition of fly ash on reduction of the size of microcracks in the ITZ of concrete composites under dynamic loading. *Energies* 14 (3):668. doi: 10/3390/en14030668.

Hou, R., and Y. Xia. 2021. Review on the new development of vibration-based damage identification for civil engineering structures: 2010-2019. *Journal of Sound and Vibration* 491:115741. doi: 10.1016/j.jsv.2020.115741.

Hu, Y., and X. Zhang. 2011. Parametric vibration and stability of a functionally graded plate. *Mechanics Based Design of Structures and Machines* 39 (3):367–77.

Huang, G., F. Song, and X. Wang. 2010. Quantitative modeling of coupled piezo-elastodynamic behavior of piezoelectric actuators bonded to an elastic medium for structural health monitoring: a review. *Sensors (Basel, Switzerland)* 10 (4):3681–702. doi: 10.3390/s100403681.

Khiem, N. T., T. T. Hai, and L. Q. Huong. 2020. Effect of piezoelectric patches on natural frequencies of Timoshenko beam made of functionally graded. *Materials Research Express* 7 (5):055704. doi: 10.1088/2053-1591/ab8df5.

Khiem, N. T., and N. N. Huyen. 2017. A method for crack identification in functionally graded Timoshenko beam. *Nondestructive Testing and Evaluation* 32 (3):319–41. doi: 10.1080/10589759.2016.1226304.

Khiem, N. T., N. N. Huyen, and N. T. Long. 2017. Vibration of cracked Timoshenko beam made of functionally graded material. *Shock & Vibration, Aircraft/Aerospace, Energy Harvesting, Acoustics & Optics* 9 (15):133–43.

Khiem, N. T., H. T. Tran, and D. Nam. 2020. Modal Analysis of cracked continuous Timoshenko beam made of functionally graded material. *Mechanics Based Design of Structures and Machines* 48 (4):459–79. doi: 10.1080/15397734.2019.1639518.

Khorramabadi, M. K., and A. R. Nezamabadi. 2010. Stability of functionally graded beams with piezoelectric layers based on the first order shear deformation theory. *International Journal of Electrical and Computer Engineering* 4 (11):1641–4.

Kim, K.,. S. Kim, K. Sok, C. Pak, and K. Han. 2018. A modeling method for vibration analysis of cracked beam with arbitrary boundary conditions. *Journal of Ocean Engineering and Science* 3 (4):367–81. doi: 10.1016/j.joes.2018.11.003.

Larbi, L. O., A. Kaci, M. S. A. Houari, and A. Tounsi. 2013. An efficient shear deformation beam theory based on neutral surface position for bending and free vibration of functionally graded beams. *Mechanics Based Design of Structures and Machines* 41 (4):421–33. doi: 10.1080/15397734.2013.763713.

Li, X. F. 2008. A unified approach for analyzing static and dynamic behaviors of functionally graded Timoshenko and Euler-Bernoulli beams. *Journal of Sound and Vibration* 318 (4-5):1210–29. doi: 10.1016/j.jsv.2008.04.056.

Li, Y. S., W. J. Feng, and Z. Y. Cai. 2014. Bending and free vibration of functionally graded piezoelectric beam based on modified strain gradient. *Composite Structures* 115:41–50. doi: 10.1016/j.compstruct.2014.04.005.

Na, W. S., and J. Baek. 2018. A review of the piezoelectric electromechanical impedance based structural health monitoring technique for engineering structures. *Sensors* 18 (5):1307. doi: 10.3390/s18051307.

Park, G., H. Sohn, C. R. Farrar, and D. I. Inman. 2003. Overview of piezoelectric Impedance-based Health Monitoring and Path Forward. *The Shock and Vibration Digest* 35 (6):451–63. doi: 10.1177/05831024030356001.

Rao, S. S., and M. Sunar. 1994. Piezoelectricity and its use in disturbance sensing and control of flexible structures: A Survey. *Applied Mechanics Reviews* 47 (4):113–23. doi: 10.1115/1.3111074.

Ritdumrongkul, S., and Y. Fujino. 2007. Identification of the location and size of cracks in beam by piezoelectric actuator-sensor. *Structural Control and Health Monitoring* 14 (6):931–43. doi: 10.1002/stc.204.

Shu, Z. 2017. Application of piezoelectric material in structural health monitoring of civil engineering structure. *Chemical Engineering Transaction* 59:523–8. doi: 10.3303/CET1759088.

Sina, S. A., H. M. Navazi, and H. Haddadpour. 2009. An analytical method for free vibration analysis of functionally graded beams. *Materials and Design.* 30 (3):741–7. doi: 10.1016/j.matdes.2008.05.015.

Sohn, H., C. R. Farrar, F. M. Hemez, D. D. Shunk, D. W. Stinemates, and B. R. Nadler. 2003. A review of structural health monitoring literature: 1996–2001, Los Alamos National Laboratory Report, USA.

Su, H., and J. R. Banerjee. 2015. Development of dynamic stiffness method for free vibration of functionally graded Timoshenko beam. *Computers & Structures* 147:107–16. doi: 10.1016/j.compstruc.2014.10.001.

Tzou, H. S., and C. I. Tseng. 1990. Distributed piezoelectric sensor/actuator design for dynamic measurement/control of distributed parameter systems: A piezoelectric finite element approach. *Journal of Sound and Vibration* 138 (1):17–34. doi: 10.1016/0022-460X(90)90701-Z.

Viola, E., A. Marzani, and N. Fantuzzi. 2016. Interaction effect of cracks on flutter and divergence instabilities of cracked beams under subtangential force. *Engineering Fracture Mechanics* 151:109–29. doi: 10.1016/j.engfracmech.2015.11.010.

Viola, E., L. Nobile, and L. Federici. 2002. Formulation of cracked beam element for structural analysis. *Journal of Engineering Mechanics* 128 (2):220–30. doi: 10.1061/(ASCE)0733-9399(2002)128:2(220).

Wang, Q., W. H. Duan, and S. T. Quek. 2004. Repair of notched beam under dynamic load using piezoelectric patch. *International Journal of Mechanical Sciences* 46 (10):1517–33. doi: 10.1016/j.ijmecsci.2004.09.012.

Wang, X., X. Liang, and C. Jin. 2017. Accurate dynamic analysis of functionally graded beams under a moving point load. *Mechanics Based Design of Structures and Machines* 45 (1):76–91. doi: 10.1080/15397734.2016.1145060.

Wang, Q., and S. T. Quek. 2000. Flexural vibration analysis of sandwich beam coupled with piezoelectric actuator. *Smart Materials and Structures* 9 (1):103–9. doi: 10.1080/15397734.2013.763713.

Wang, Q., and S. T. Quek. 2002. Enhancing flutter and buckling capacity of column by piezoelectric layers. *International Journal of Solids and Structures*39 (16):4167–80. doi: 10.1016/S0020-7683(02)00334-7.

Wang, D. S., H. Y. Song, and H. P. Zhu. 2015. Electromechanical impedance analysis on piezoelectric smart beam with a crack based on spectral element method. *Mathematical Problems in Engineering* 2015:713501 doi: 10.1155/2015/713501.

Wang, T., B. Tan, M. Lu, Z. Zhang, and G. Lu. 2020. Piezoelectric Electro-Mechanical Impedance (EMI) Based Structural Crack Monitoring. *Applied Sciences* 10 (13):4648. doi: 10.3390/app10134648.

Winston, H. A., F. Sun, and B. S. Annigeri. 2000. Structural Health Monitoring with Piezoelectric Active Sensors. Procc. ASME Turbo Expo 2000, May 8-11, 2000, Munich, Germany. doi: 10.1115/2000-GT-0051.

Yang, J., and Y. Chen. 2008. Free vibration and buckling analyses of functionally graded beams with edge cracks. *Composite Structures* 83 (1):48–60. doi: 10.1016/j.compstruct.2007.03.006.

Yu, Z. G., and F. L. Chu. 2009. Identification of crack in functionally graded material beams using the *p*-version of finite element method. *Journal of Sound and Vibration* 325 (1-2):69–84. doi: 10.1016/j.jsv.2009.03.010.

Zhao, S., M. Wu, and Q. Wang. 2017. Crack identification through scan-tuning of vibration characteristics using piezoelectric material. *Smart Materials and Structures* 26 (2):025005. doi: 10.1088/1361-665X/aa520a.